Autonomous Movement of Controllable Assembled Janus Capsule Motors

Yingjie Wu,[†] Zhiguang Wu,[†] Xiankun Lin,[†] Qiang He,[†,*] and Junbai Li[‡,*]

[†]Key Laboratory of Microsystems and Microstructures Manufacturing, Ministry of Education, Micro/Nanotechnology Research Centre, Harbin Institute of Technology, Yi Kuang Jie 2, Harbin 150080, China and [‡]Institute of Chemistry, Chinese Academy of Sciences, Zhong guan cun Bei yi jie 2, Beijing 100190, China

ABSTRACT We demonstrate the first example of a self-propelled Janus polyelectrolyte multilayer hollow capsule that can serve as both autonomous motor and smart cargo. This new autonomous Janus capsule motor composed of partially coated dendritic platinum nanoparticles (Pt NPs) was fabricated by using a template-assisted layer-by-layer (LbL) self-assembly combined with a microcontact printing method. The resulting Janus capsule motors still retain outstanding delivery capacities and can respond to external stimuli for controllable encapsulation and triggered release of model drugs. The Pt NPs on the one side of the Janus capsule motors catalytically decompose hydrogen peroxide fuel, generating oxygen bubbles which then recoil the movement of the capsule motors in solution or at an interface. They could autonomously move at a maximum speed of above 1 mm/s (over 125 body lengths/s), while exerting large forces exceeding 75 pN. Also, these asymmetric hollow capsules can be controlled by an external magnetic field to achieve directed movement. This LbL-assembled Janus capsule motor system has potential in making smart self-propelling delivery systems.

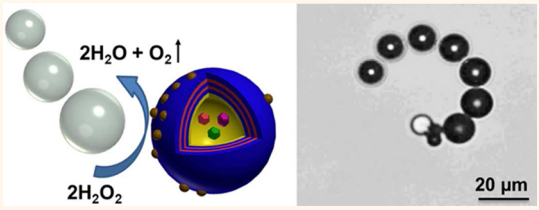

KEYWORDS: layer-by-layer assembly · Janus capsule · autonomous motor · smart cargo · bubble propulsion

Engineering artificial micro/nanomachines which catalytically harness the chemical energy in their environment to move autonomously has recently attracted considerable interest.[1−5] Potential applications of these micro/nanomachines include targeted drug delivery, separation, biosensing, fabrication of active biomimetic systems, and other emerging applications.[6−10] Whitesides *et al.* first demonstrated the concept of an autonomous motor in 2002. They prepared macroscopic plates capable of converting chemical energy into autonomous motion because of the momentum of bubbles generated at the platinum (Pt) catalyst sites.[11] Since then, a number of excellent studies have been published on the design of powerful artificial motors on the micro- and nanoscale such as bimetallic nanorods,[12,13] metallic and dielectric particles,[14,15] and tubular catalytic microengines.[16−21] Depending on the systems, several mechanisms were proposed to explain the motor motion, such as bubble propulsion, interfacial tension gradients, self-electrophoresis, self-diffusiophoresis, and Brownian ratchet.[22−26] These chemically powered man-made motors can be used to pick up, transport, and release various cargoes including polymer particles,[27−29] nucleic acids,[30] cancer cells,[18] bacteria,[31] and liposomes[32] *via* electrostatic, chemical, or magnetic interactions. In many cases, extra functionalities of micro/nanomotors have to be made (*e.g.*, magnetic properties, special chemical modifications, or treatment) in order to pick up or release cargoes. Despite these advances in man-made chemically catalytic motor systems, there are still many inherent limitations, such as complex preparation technology, expensive equipment, difficulty of surface modification, and poor biocompatibility or biodegradability. Particularly, these motors need the postmodification or complex operation for loading various cargoes and delivering functional components, but cannot encapsulate targeted substances by themselves in an easy and controllable way. Therefore, the easy loading and delivery of cargo or integration of autonomous motor and smart cargo into a smart system remains a big challenge.

For such a smart system, layer-by-layer (LbL) self-assembled polyelectrolyte hollow capsules should be excellent candidates.[33−39] They can be readily prepared by the consecutive adsorption of alternating layers of

* Address correspondence to qianghe@hit.edu.cn, jbli@iccas.ac.cn.

Received for review September 19, 2012 and accepted November 15, 2012.

Published online November 15, 2012
10.1021/nn304335x

positively and negatively charged polyelectrolytes onto sacrificial colloidal particles. It was shown that the LbL-assembled capsules possess outstanding delivery capacities and can respond to various stimuli for controllable encapsulation and release of drugs or other components,[40−47] but until now not in connection with autonomous motor systems. Herein, we expect that the first demonstration of highly efficient and controllable autonomous LbL-assembled capsules will open the door to powerful vehicle systems, performing drug encapsulation and release, and active transportation without the need of external resources.

In this study we choose the catalytic decomposition of hydrogen peroxide fuel to oxygen and water, providing power for new LbL-assembled capsule motors. Platinum nanoparticles (Pt NPs) are used as catalyst because they could function as protein mimics and have relatively high stability and catalytic efficiency.[48] In view of this, a key step to effectively power these LbL-assembled capsule motors is to generate the unidirectional resultant forces through an asymmetric modification of catalysts. This asymmetric modification of catalysts on the capsule surface enables control of the speed and direction of the capsule motor motion in a defined manner. In this case, the microcontact printing technique can easily be employed to prepare Pt NP-functionalized capsules with controllable anisotropy (patchiness) (*i.e.*, so-called Janus structure). We here show that these resulting Janus capsules can self-propel at a high speed of more than 1 mm/s (over 125 body lengths/s) at 30% H_2O_2 and can move at a very low fuel level down to 1% H_2O_2. The ultrafast motion of capsule motors reflects the enhanced catalytic decomposition of the dendritic Pt NP functionalized surface.

RESULTS AND DISCUSSION

Five bilayers of polystyrene sulfonate (PSS)/polyallylamine hydrochloride (PAH) were deposited on the surface of 8 μm silica particles *via* the LbL assembly according to the procedures previously reported (see Supporting Information (SI)).[33,49] Next, a PDMS stamp loaded with a dendritic Pt NP ink was placed on top of the $(PSS/PAH)_5$-coated particle monolayer for several seconds (Figure 1A). After removal of the silica templates, hollow asymmetric capsules modified with Pt NPs were obtained. Transmission electron microscopy (TEM, Figure 1B, SI Figure S1F), scanning electron microscopy (SEM, SI Figure S1B and S1E), and atomic force microscopy (AFM, SI Figure S1C) reveal the successful preparation of dendritic Pt NP-functionalized asymmetric capsules. The dendritic Pt NPs with a diameter of about 200 nm are mainly distributed on one side of the capsules. The presence of both carbon (from polyelectrolytes) and Pt in the resulting asymmetric capsules was also confirmed by energy-dispersive X-ray (EDX) spectroscopy (SI Figure 1G).

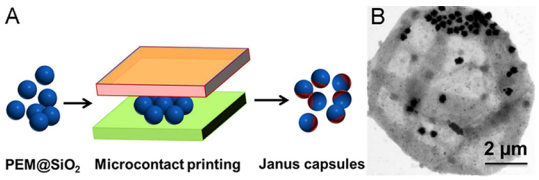

Figure 1. (A) Schematic representation of the fabrication of Pt NP-modified asymmetric polyelectrolyte capsules *via* microcontact printing. (B) TEM image of dendritic Pt NP-functionalized $(PSS/PAH)_5$ capsule after the removal of the template.

We and other researchers have proved that LbL-assembled polyelectrolyte multilayer capsules are smart cargoes which could encapsulate and release targeted materials in a controlled manner.[33−40,49,50] For instance, chemical (ionic strength, pH, electrochemical and solvent), physical (temperature, laser light, electric and magnetic field, ultrasound, and mechanical action), and biological (enzymes and receptors) stimuli of as-assembled capsules have been widely studied.[41−47] As a test, we performed the encapsulation and release of a model component, fluorescein isothiocyanate-dextrans (FITC-dextran), using an organic solvent to selectively tune the permeability of LbL-assembled capsules.[42] So they can be observed in a fluorescence microscope, the capsules were assembled using Rhodamine-labeled PAH, and thus the red circles in the confocal laser scanning microscopy (CLSM) image (Figure 2A,D) represent the capsule wall. When FITC-dextran was incubated with $(PSS/PAH)_5$ capsule solution, the capsule wall remains in a closed state and is not permeable for FITC-dextran. In contrast, the capsule wall remains in an open state after the addition of ethanol, and the FITC-dextran can enter into the capsule. Green fluorescence of the interior of the capsules in Figure 2B confirms the successful encapsulation of the model compound FITC-dextran. Following a similar mechanism, FITC-dextran could be released rapidly by adding ethanol as illustrated in Figure 2D,E,F.

The autonomous movement of dendritic Pt NP-modified asymmetric capsule motors was recorded by optical microscopy. Typical time-lapse images are shown in Figure 3A,C and their original videos (SI videos 1 and 2). Correspondingly, Figure 3B,D show the tracking trajectories of two capsule motors. One can see that the capsule motors rapidly swim by bubble propulsion, and have two typical kinds of moving trajectories, circular (Figure 3A, SI video 1) and spiral (Figure 3C, SI video 2) motion in a 15% H_2O_2 solution at a speed of about 140 μm/s (18 body lengths/s) and 110 μm/s (14 body lengths/s), respectively. The different trajectories are presumably due to the different size and shape of the adsorbed Pt NP patches as well as the LbL assembled capsules. Similar moving trajectories were previously reported for large rolled-up microengines,[10] electrosynthesized polyaniline/Pt microtubes,[20] and Pt NP-loaded polymersomes.[51] It is important to note that the speed of the capsules' motion is very rapid along a

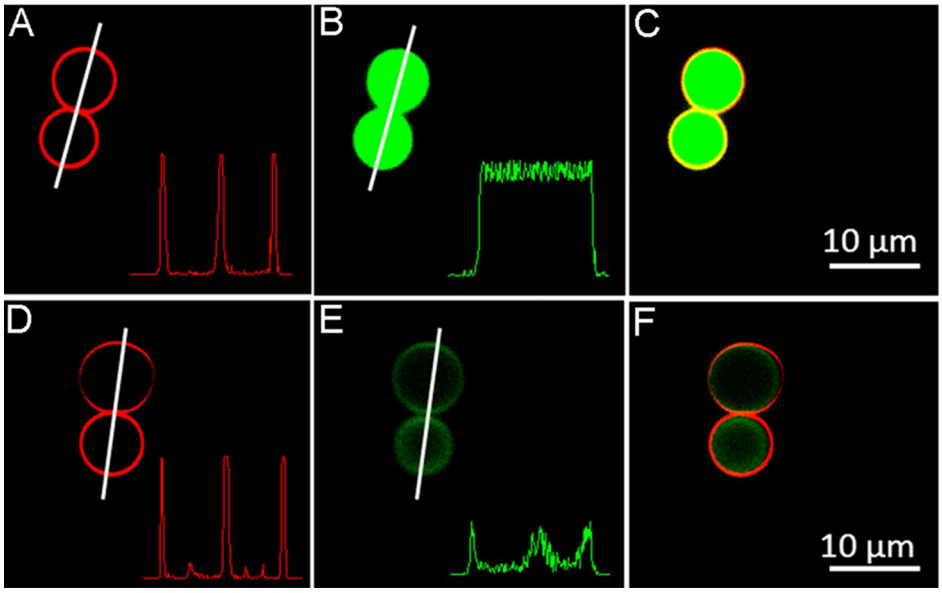

Figure 2. Confocal laser scanning microscopy (CLSM) images of LbL-assembled $(PSS/PAH)_5$ capsules (A,B,C) encapsulated with and (D,E,F) released a model component FITC-dextran. (A,D) FITC channel; (B,E) TRITC channel; (C,F) overlap of FITC channel and TRITC channel. The outer polyelectrolyte shell of the $(PSS/PAH)_5$ capsule is TRITC-PAH; the inside was loaded with FITC-dextran.

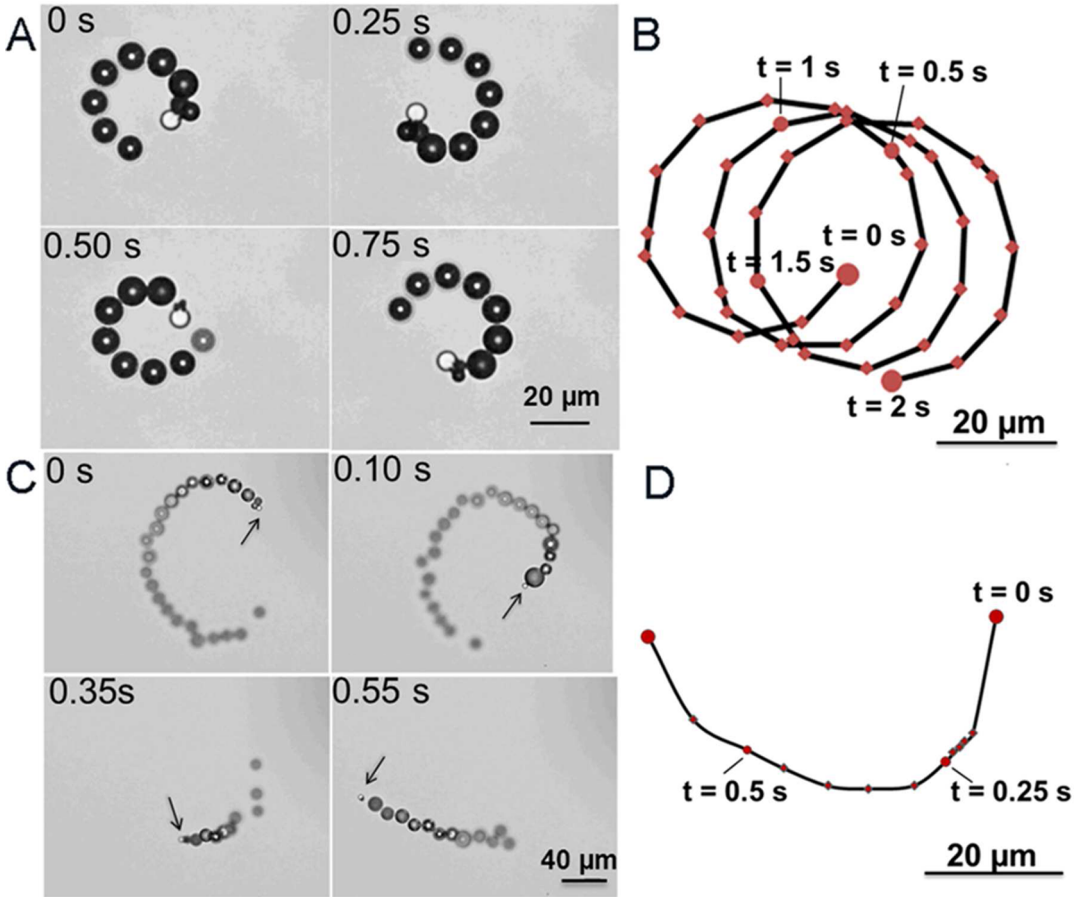

Figure 3. High-speed motion of the $(PSS/PAH)_5$ capsule motors at 15% H_2O_2. Consecutive time frames obtained in an optical microscope displaying (A) circular motion and (C) spiral motion. (B,D) Trajectories of the two typical kinds of capsule motion. Here, the white dot means capsule motor and the dark bubbles after the white dot represent the oxygen bubble tails.

linear path but obviously decreases once they change the movement direction as shown in Figure 3B,D. In addition, these self-assembled capsule motors in the aqueous H_2O_2 solution can continue their movement

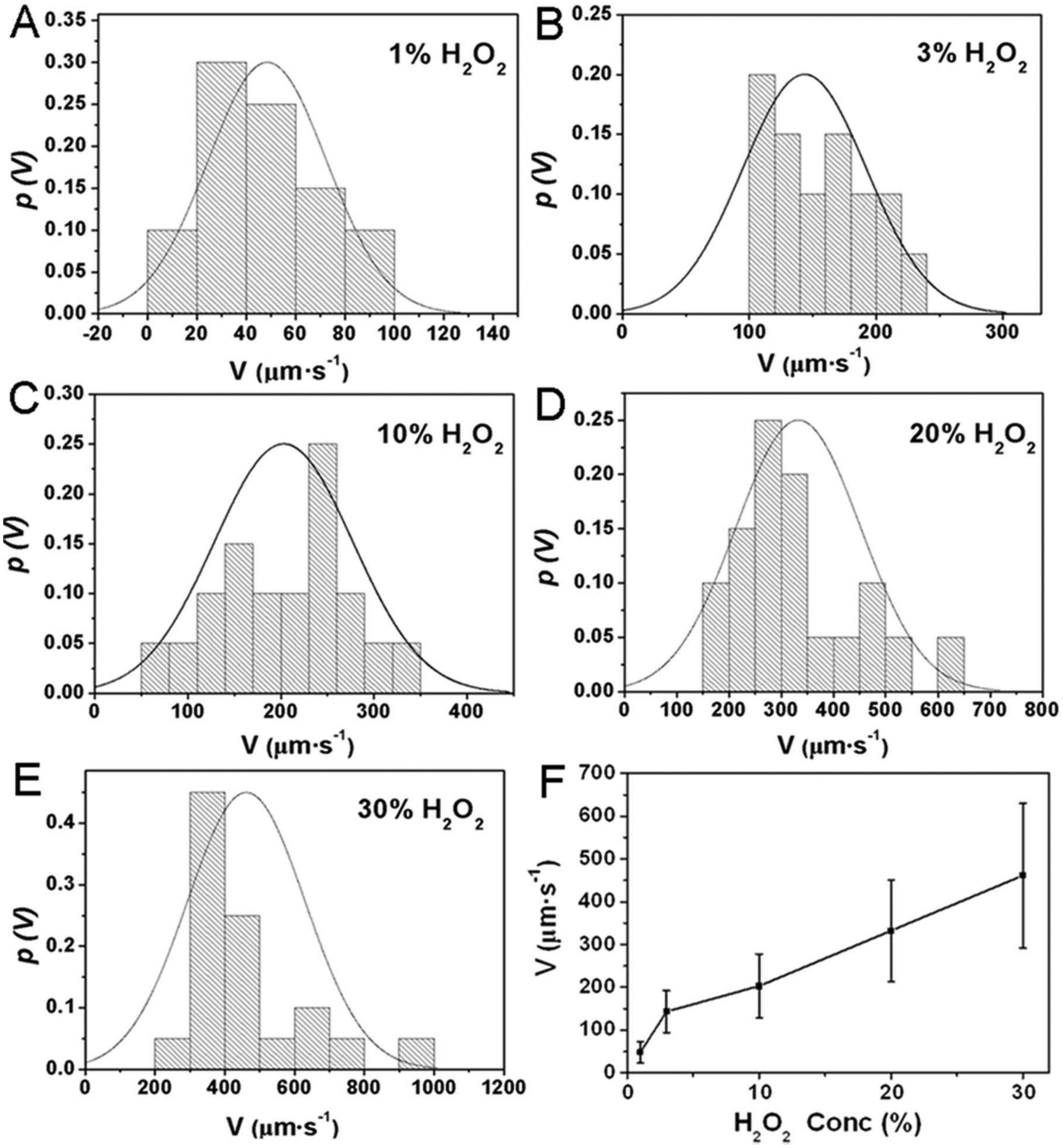

Figure 4. Histograms and Gaussian fit curves of the velocity (*V*) of the $(PSS/PAH)_5$ capsule motors for different fuel concentrations: (A) 1%; (B) 3%; (C) 10%; (D) 20%; (E) 30% H_2O_2. (F) Comparison of average speed distribution of the motors.

without obvious deceleration beyond 30 min, traveling distances greater than 30 cm.

Furthermore, the velocity of the catalytic capsule motors can be readily modulated through a change in the concentration of the hydrogen peroxide fuel. Figure 4 shows histograms representation of the speed distribution of Pt NP-functionalized LbL-assembled capsule motors in different fuel concentrations ranging from 1% to 30%. We can see that the average speed of the capsule motors increases from ~50 μm/s at 1% H_2O_2 (over 6 body lengths/s, see SI video 3) to ~480 μm/s at 30% H_2O_2 (60 body lengths/s, see SI video 4). More interestingly, dendritic Pt NP-functionalized asymmetric capsule motors at low H_2O_2 concentration (below 3%) display a much faster speed than the Pt-coated asymmetric silica microparticle motors.[52] Furthermore, the capsule motors can self-propel at a top speed of about 1 mm/s (125 body lengths/s) under aqueous 30% H_2O_2 solution (Figure 4E), and obviously move faster than the reported Janus silica or rolled-up tubular microengines in a similar H_2O_2 fuel concentration.[10,52] The average rate of the LbL-assembled capsule motors significantly increases with the increase of the H_2O_2 concentration over a 1−30% range without the presence of any other surfactants, indicating a substantial enhancement of the fuel consumption rate and reflecting the high catalytic activity of dendritic Pt NPs toward hydrogen peroxide decomposition. Such pronounced speeds should be derived from the asymmetric distribution and high catalytic efficiency of dendritic Pt NPs on the surface of LbL-assembled capsules. It has been proved that the dendritic structure of Pt NPs has a larger specific surface area and a higher catalytic reactivity compared to

smooth Pt films.[53] Hence, our active assembled systems only need a small fraction of Pt component to catalytically drive the rapid motion of the capsule motors, and thus could move in a roughly controllable speed which is based on the dependence of the capsule motor speed upon the fuel concentration.

Assuming that the forces exerted by the asymmetric capsule motors are equal to the hydrodynamic drag forces at a steady state, the driving force of single spherical capsule motor is thus approximately proportional to its velocity at small Reynolds numbers and can be estimated using the Stokes law.[54]

$$F_{drag} = 6\pi\mu rv$$

where v is the capsule velocity, μ is the fluid viscosity, and r is the radius of the capsule. The Stokes drag force for one capsule running at a maximum velocity of 1 mm/s is thus calculated to be about 75 pN. It means that a capsule could be loaded with a maximum quality of about 7.65 ng. In other words, these LbL-assembled capsule motors can indeed serve as both powerful motor and smart cargo because these capsule motor systems are inherently multifunctional as demonstrated in Figure 2. Furthermore, Supporting Information, Figure S2 and its corresponding video (SI video 5) show the rapid transportation of a FITC-dextran loaded capsule motor in a 15% H_2O_2 solution. As expected, these capsules show pronounced movement without leaking of FITC-dextrans and subsequently FITC-dextrans could be released from capsules in several seconds by adding ethanol.

The above-mentioned capsule motors move randomly; it is also possible to guide them magnetically by assembling negatively charged magnetic nanoparticles into the capsule wall. Time-lapse pictures of the motion of a single capsule motor under a magnetic field in 15% H_2O_2 solution are shown in Figure 5 (taken from SI video 6). One can see that the capsule started to swim toward the direction of an external magnetic field. Furthermore, the guided motion of a swarm of capsule motors was also provided in SI video 7. The magnetically guided directional motion of capsule motors can be conveniently performed and is of significant importance for the design of more powerful nanomachines.

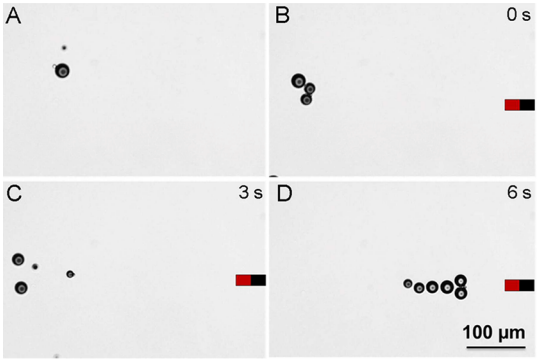

Figure 5. Control of the direction of $(PSS/PAH)_5$ capsule motor movement by applying an external magnetic field at 15% H_2O_2. A ferromagnet was placed on the right side of the motors.

CONCLUSIONS

We have developed a dendritic Pt NP-functionalized asymmetric capsule motor through the LbL self-assembly combined with microcontact printing. These autonomous capsule motors could be rapidly propelled by oxygen bubbles and only need a small number of dendritic Pt NPs with high catalytic efficiency. More importantly, our assembled capsules can thus serve as both efficient catalytic motor and smart cargo. This makes them extremely attractive especially toward the design of more powerful nanomachines and diverse biomedical applications.

EXPERIMENTAL SECTION

Materials. The silica spheres with the diameter of 8 μm were obtained from Microparticles GmbH, Berlin, Germany. Poly(styrenesulfonate) sodium salt (PSS, M_w = 70 000), poly(allylamine hydrochloride) (PAH, M_w = 70 000), poly(diallyldimethylammonium chloride) (PDDA, 20 wt % in water, M_w = 100 000−200 000), fluorescein isothiocyanate-dextran (FITC-dextran, average molwt 3000−5000), tetramethylrhodamine-isothiocyanate (TRITC), and fluorescein isothiocyanate (FITC) were purchased from Sigma-Aldrich. Chloroplatinic acid (H_2PtCl_6), sodium chloride (NaCl), hydrofluoric acid (HF), and hydrogen peroxide (H_2O_2) were obtained from Beijing Chemical Works, China. TRITC-modified PAH (TRITC-PAH) was prepared through labeling PAH with TRITC according to the literature.[49] All commercial materials were used without further purification.

Preparation of Dendritic Pt NP-Functionalized Asymmetric LbL-Assembled Capsules. $(PSS/PAH)_5$-coated particles were first prepared by the layer-by-layer assembly of polyelectrolyte layers on the surface of SiO_2 particles with a diameter of 8 μm. The SiO_2 particles were suspended in 2 mg/mL PAH solution containing 0.5 M NaCl for 15 min under continuous shaking. Excess polyelectrolytes were removed by centrifugation and washing three times using 0.1 M NaCl. The PAH-adsorbed silica particles were then suspended in 2 mg/mL PSS solution containing 0.5 M NaCl for 15 min under continuous shaking, followed by three repeated centrifugation/washing steps. The $(PSS/PAH)_5$-coated silica particles were obtained by repeating the above deposition procedure and the outer layer was PSS. Citrate-stabilized magnetic iron oxide nanoparticles (negative charged) and PDDA-stabilized dendritic platinum particles (positive charged) were synthesized according to previous reports.[55] Next, dendritic Pt NPs were assembled on the top surface of $(PSS/PAH)_5$-coated particle monolayers by using microcontact printing.[45] The silica cores were then dissolved by treatment with 1 M HF (Caution: *HF is extremely toxic and can penetrate the skin*!). The Janus capsules were purified by three centrifugation/water washing steps. To magnetically operate the movement direction of the capsule motors, citrate-stabilized magnetic iron oxide nanoparticles with an average diameter of 15 nm were assembled into the multilayer of the $(PSS/PAH)_5$-coated particles before the assembly of Pt NPs by using a microcontact printing method. All obtained capsule solutions were stored at 4 °C.

Encapsulation and Release of a Model Drug. A solvent-controlled precipitation method was used for the encapsulation of a model drug, fluorescein isothiocyanate-dextrans (FITC-dextran).[42] At first, dendritic Pt NP-modified hollow capsules were exposed to

a FITC-dextran-containing (10 mg/mL) water/ethanol mixture (1:1, v/v) which made the capsule shell permeable toward FITC-dextran molecules. Then excess FITC-dextran and ethanol was washed out with water and the FITC-dextran molecules were captured inside the polyelectrolyte capsules. Correspondingly, the encapsulated FITC-dextran was rapidly released in several seconds once the capsules were exposed to a water/ethanol mixture (1:1, v/v).

Analysis of the Motion of Capsule Motors. Movement studies were performed by adding equal volumes of diluted Janus micromotor solution into hydrogen peroxide fuel solution with different concentration (v/v, 1−30%), and actual videos were taken after 2 min. To magnetically operate the capsule motor, an external weak magnetic field was applied by placing a small magnet at 10 cm away from the glass slide without changing the distances. All optical microscope images of the micromotor movement were tracked using the Metamorph tracking module, and the results were analyzed using Origin Pro 7.5 software.

Characterization. An Olympus BX53 fluorescence microscope was employed to record the motion of capsule motors. For SEM (Hitachi S-5200) and AFM (Agilent 5400AFM) observation, a drop of sample solution was dropped onto a silicon wafer with sequential drying at room temperature overnight. TEM was performed using a Tecnai G2 F30 microscope. Copper grids sputtered with carbon films were used to support the sample. Fluorescence images were obtained using a Leica TCS SP5 II CLSM. The excitation wavelength was 488 and 532 nm.

Conflict of Interest: The authors declare no competing financial interest.

Supporting Information Available: Additional figures and videos as described in the text. This material is available free of charge *via* the Internet at http://pubs.acs.org.

Acknowledgment. The authors thank Prof. H. Moehwald for useful discussion and consistent support. This work was supported by the National Nature Science Foundation of China (91027045), 100-talent Program of HIT, and New Century Excellent Talent Program (NCET-11-0800).

REFERENCES AND NOTES

1. van den Heuvel, M. G. L.; Dekker, C. Motor Proteins at Work for Nanotechnology. *Science* **2007**, *317*, 333–336.
2. Kinbara, K.; Aida, T. Toward Intelligent Molecular Machines: Directed Motions of Biological and Artificial Molecules and Assemblies. *Chem. Rev.* **2005**, *105*, 1377–1400.
3. Ozin, G. A.; Manners, I.; Fournier-Bidoz, S.; Arsenault, A. Dream Nanomachines. *Adv. Mater.* **2005**, *17*, 3011–3018.
4. Wang, J. Can Man-Made Nanomachines Compete with Nature Biomotors? *ACS Nano* **2009**, *3*, 4–9.
5. Mei, Y. F.; Solovev, A. A.; Sanchez, S.; Schmidt, O. G. Rolled-Up Nanotech on Polymers: From Basic Perception to Self-Propelled Catalytic Microengines. *Chem. Soc. Rev.* **2011**, *40*, 2109–2119.
6. Wang, J.; Gao, W. Nano/Microscale Motors: Biomedical Opportunities and Challenges. *ACS Nano* **2012**, *6*, 5745–5751.
7. Kline, T. R.; Paxton, W. F.; Mallouk, T. E.; Sen, A. Catalytic Nanomotors: Remote-Controlled Autonomous Movement of Striped Metallic Nanorods. *Angew. Chem., Int. Ed.* **2005**, *44*, 744–746.
8. Paxton, W. F.; Kistler, K. C.; Olmeda, C. C.; Sen, A.; Angelo, S. K. S.; Cao, Y.; Mallouk, T. E.; Lammert, P. E.; Crespi, V. H. Catalytic Nanomotors: Autonomous Movement of Striped Nanorods. *J. Am. Chem. Soc.* **2004**, *126*, 13424–13431.
9. Fournier-Bidoz, S.; Arsenault, A. C.; Manners, I.; Ozin, G. A. Synthetic Self-Propelled Nanorotors. *Chem. Commun.* **2005**, *4*, 441–443.
10. Mei, Y. F.; Huang, G. S.; Solovev, A. A.; Ureña, E. B.; Mönch, I.; Ding, F.; Reindl, T.; Fu, R. K. Y.; Chu, P. K.; Schmidt, O. G. Versatile Approach for Integrative and Functionalized Tubes by Strain Engineering of Nanomembranes on Polymers. *Adv. Mater.* **2008**, *20*, 4085–4090.
11. Ismagilov, R. F.; Schwartz, A.; Bowden, N.; Whitesides, G. M. Autonomous Movement and Self-Assembly. *Angew. Chem., Int. Ed.* **2002**, *41*, 652–654.
12. Dhar, P.; Fischer, Th. M.; Wang, Y.; Mallouk, T. E.; Paxton, W. F.; Sen, A. Autonomously Moving Nanorods at a Viscous Interface. *Nano Lett.* **2006**, *6*, 66–72.
13. Sundararajan, S.; Lammert, P. E.; Zudans, A. W.; Crespi, V. H.; Sen, A. Catalytic Motors for Transport of Colloidal Cargo. *Nano Lett.* **2008**, *8*, 1271–1276.
14. Howse, J. R.; Jones, R. A. L.; Ryan, A. J.; Gough, T.; Vafabakhsh, R.; Golestanian, R. Self-Motile Colloidal Particles: From Directed Propulsion to Random Walk. *Phys. Rev. Lett.* **2007**, *99*, 048102.
15. Gibbs, J. G.; Kothari, S.; Saintillan, D.; Zhao, Y. P. Geometrically Designing the Kinematic Behavior of Catalytic Nanomotors. *Nano Lett.* **2011**, *11*, 2543–2550.
16. Solovev, A. A.; Mei, Y. F.; Ureña, E. B.; Huang, G. S.; Schmidt, O. G. Catalytic Microtubular Jet Engines Self-Propelled by Accumulated Gas Bubbles. *Small* **2009**, *5*, 1688–1692.
17. Sanchez, S.; Solovev, A. A.; Mei, Y. F.; Schmidt, O. G. Dynamics of Biocatalytic Microengines Mediated by Variable Friction Control. *J. Am. Chem. Soc.* **2010**, *132*, 13144–13145.
18. Balasubramanian, S.; Kagan, D.; Hu, C.M. J.; Campuzano, S.; Lobo-Castañon, M. J.; Lim, N.; Kang, D. Y.; Zimmerman, M.; Zhang, L. F.; Wang, J. Micromachine-Enabled Capture and Isolation of Cancer Cells in Complex Media. *Angew. Chem., Int. Ed.* **2011**, *50*, 4161–4164.
19. Orozco, J.; Campuzano, S.; Kagan, D.; Zhou, M.; Gao, W.; Wang, J. Dynamic Isolation and Unloading of Target Proteins by Aptamer-Modified Microtransporters. *Anal. Chem.* **2011**, *83*, 7962–7969.
20. Gao, W.; Sattayasamitsathit, S.; Orozco, J.; Wang, J. Highly Efficient Catalytic Microengines: Template Electrosynthesis of Polyaniline/Platinum Microtubes. *J. Am. Chem. Soc.* **2011**, *133*, 11862–11864.
21. Gao, W.; Uygun, A.; Wang, J. Hydrogen-Bubble-Propelled Zinc-Based Microrockets in Strongly Acidic Media. *J. Am. Chem. Soc.* **2012**, *134*, 897–900.
22. Paxton, W. F.; Sundararajan, S.; Mallouk, T. E.; Sen, A. Chemical Locomotion. *Angew. Chem., Int. Ed.* **2006**, *45*, 5420–5429.
23. Popescu, M. N.; Dietrich, S.; Tasinkevych, M.; Ralston, J. Phoretic Motion of Spheroidal Particles Due to Self-Generated Solute Gradients. *Eur. Phys. J. E.* **2010**, *31*, 351–367.
24. Ebbens, S. J.; Howse, J. R. In Pursuit of Propulsion at the Nanoscale. *Soft Matter* **2010**, *6*, 726–738.
25. Gibbs, J. G.; Zhao, Y. P. Autonomously Motile Catalytic Nanomotors by Bubble Propulsion. *Appl. Phys. Lett.* **2009**, *94*, 163104.
26. Thakur, S.; Kapral, R. Dynamics of Self-Propelled Nanomotors in Chemically Active Media. *J. Chem. Phys.* **2011**, *135*, 024509.
27. Sundararajan, S.; Sengupta, S.; Ibele, M. E.; Sen, A. Drop-Off of Colloidal Cargo Transported by Catalytic Pt−Au Nanomotors *via* Photochemical Stimuli. *Small* **2010**, *6*, 1479–1482.
28. Solovev, A. A.; Sanchez, S.; Pumera, M.; Mei, Y. F.; Schmidt, O. G. Magnetic Control of Tubular Catalytic Microbots for the Transport, Assembly, and Delivery of Micro-objects. *Adv. Funct. Mater.* **2010**, *20*, 2430–2435.
29. Baraban, L.; Makarov, D.; Streubel, R.; Mönch, I.; Grimm, D.; Sanchez, S.; Schmidt, O. G. Catalytic Janus Motors on Microfluidic Chip: Deterministic Motion for Targeted Cargo Delivery. *ACS Nano* **2012**, *6*, 3383–3389.
30. Kagan, D.; Campuzano, S.; Balasubramanian, S.; Kuralay, F.; Flechsig, G. U.; Wang, J. Functionalized Micromachines for Selective and Rapid Isolation of Nucleic Acid Targets from Complex Samples. *Nano Lett.* **2011**, *11*, 2083–2087.
31. Campuzano, S.; Orozco, J.; Kagan, D.; Guix, M.; Gao, W.; Sattayasamitsathit, S.; Claussen, J. C.; Merkoçi, A.; Wang, J. Bacterial Isolation by Lectin-Modified Microengines. *Nano Lett.* **2012**, *12*, 396–401.
32. Kagan, D.; Laocharoensuk, R.; Zimmerman, M.; Clawson, C.; Balasubramnian, S.; Kang, D.; Bishop, D.; Sattayasamitsathit, S.; Zhang, L. F.; Wang, J. Rapid Delivery of Drug Carriers Propelled and Navigated by Catalytic Nanoshuttles. *Small* **2010**, *6*, 2741–2747.

33. Donath, E.; Sukhorukov, G. B.; Caruso, F.; Davis, S. A.; Möhwald, H. Novel Hollow Polymer Shells by Colloid-Templated Assembly of Polyelectrolytes. *Angew. Chem., Int. Ed.* **1998**, *37*, 2201–2205.
34. Peyratout, C. S.; Dahne, L. Tailor-Made Polyelectrolyte Microcapsules: From Multilayers to Smart Containers. *Angew. Chem., Int. Ed.* **2004**, *43*, 3762–3783.
35. Such, G. K.; Johnston, A. P. R.; Caruso, F. Engineered Hydrogen-Bonded Polymer Multilayers: From Assembly to Biomedical Applications. *Chem. Soc. Rev.* **2010**, *40*, 19–29.
36. De Cock, L. J.; De Koker, S.; De Geest, B. G.; Grooten, J.; Vervaet, C.; Remon, J. P.; Sukhorukov, G. B.; Antipina, M. N. Polymeric Multilayer Capsules in Drug Delivery. *Angew. Chem., Int. Ed.* **2010**, *49*, 6954–6973.
37. He, Q.; Cui, Y.; Li, J. B. Molecular Assembly and Application of Biomimetic Microcapsules. *Chem. Soc. Rev.* **2009**, *38*, 2292–2303.
38. Hammond, P. T. Form and Function in Multilayer Assembly: New Applications at the Nanoscale. *Adv. Mater.* **2004**, *16*, 1271–1293.
39. Ariga, K.; Lvov, Y. M.; Kawakami, K.; Ji, Q. M.; Hill, J. P. Layer-by-Layer Self-Assembled Shells for Drug Delivery. *Adv. Drug Delivery Rev.* **2011**, *63*, 762–771.
40. Kharlampieva, E.; Kozlovskaya, V.; Sukhishvili, S. A. Layer-by-Layer Hydrogen-Bonded Polymer Films: From Fundamentals to Applications. *Adv. Mater.* **2009**, *21*, 3053–3065.
41. Delcea, M.; Möhwald, H.; Skirtach, A. G. Stimuli-Responsive LbL Capsules and Nanoshells for Drug Delivery. *Adv. Drug Delivery Rev.* **2011**, *63*, 730–747.
42. Lvov, Y.; Antipov, A. A.; Mamedov, A.; Möhwald, H.; Sukhorukov, G. B. Urease Encapsulation in Nanoorganized Microshells. *Nano Lett.* **2001**, *1*, 125–128.
43. Li, Z. F.; Lee, D.; Rubner, M. F.; Cohen, R. E. Layer-by-Layer Assembled Janus Microcapsules. *Macromolecules* **2005**, *38*, 7876–7879.
44. De Geest, B. G.; De Koker, S.; Sukhorukov, G. B.; Kreft, O.; Parak, W. G.; Skirtach, A. G.; Demeester, J.; De Smedt, S. C.; Hennink, W. E. Polyelectrolyte Microcapsules for Biomedical Applications. *Soft Matter* **2009**, *5*, 282–291.
45. Skirtach, A. G.; Muñoz-Javier, A.; Kreft, O.; Köhler, K.; Piera Alberola, A.; Möhwald, H.; Parak, W. J.; Sukhorukov, G. B. Laser-Induced Release of Encapsulated Materials inside Living Cells. *Angew. Chem., Int. Ed.* **2006**, *45*, 4612–4617.
46. Volodkin, D. V.; Madaboosi, N.; Blacklock, J.; Skirtach, A. G.; Möhwald, H. Surface-Supported Multilayers Decorated with Bio-active Material Aimed at Light-Triggered Drug Delivery. *Langmuir* **2009**, *25*, 14037–14043.
47. Tong, W. J.; Gao, C. Y. Multilayer Microcapsules with Tailored Structures for Bio-Related Applications. *J. Mater. Chem.* **2008**, *18*, 3799–3812.
48. Kotov, N. A. Inorganic Nanoparticles as Protein Mimics. *Science* **2010**, *330*, 188–189.
49. Duan, L.; He, Q.; Wang, K. W.; Yan, X. H.; Cui, Y.; Möhwald, H.; Li, J. B. Adenosine Triphosphate Biosynthesis Catalyzed by F_oF_1 ATP Synthase Assembled in Polymer Microcapsules. *Angew. Chem., Int. Ed.* **2007**, *46*, 6996–7000.
50. He, Q.; Duan, L.; Qi, W.; Wang, K. W.; Cui, Y.; Yan, X. H.; Li, J. B. Microcapsules Containing a Biomolecular Motor for ATP Biosynthesis. *Adv. Mater.* **2008**, *20*, 2933–2937.
51. Wilson, D. A.; R. Nolte, J. M.; van Hest, J. C. M. Autonomous Movement of Platinum-Loaded Stomatocytes. *Nat. Chem.* **2012**, *4*, 268–274.
52. Pavlick, R. A.; Sengupta, S.; McFadden, T.; Zhang, H.; Sen, A. A Polymerization-Powered Motor. *Angew. Chem., Int. Ed.* **2011**, *50*, 9374–9377.
53. Lim, B.; Xia, Y. N. Metal Nanocrystals with Highly Branched Morphologies. *Angew. Chem., Int. Ed.* **2011**, *50*, 76–85.
54. Probstein, R. F. *Physicochemical Hydrodynamics, An Introduction,* 2nd ed.; John Wiley & Sons Inc.: New York, 1994.
55. Zhang, J.; Ma, J.; Wan, Y.; Jiang, J.; Zhao, X. S. Ion Irradiation-Induced Phase Transformations in δ-γ-β Phases of Sc_2O_3−ZrO_2 Mixtures. *Mater. Chem. Phys.* **2012**, *132*, 244–248.